

$D^0 - \bar{D}^0$ Mixing in Gauge-Higgs Unification

Yuki Adachi, Nobuaki Kurahashi*, C. S. Lim* and Nobuhito Maru**

Department of Sciences, Matsue College of Technology, Matsue 690-8518, Japan

**Department of Physics, Kobe University, Kobe 657-8501, Japan*

***Department of Physics, Chuo University, Tokyo 112-8551, Japan¹*

Abstract

We discuss flavor mixing and resulting Flavor Changing Neutral Current (FCNC) in the $SU(3) \otimes SU(3)_{\text{color}}$ gauge-Higgs unification. As the FCNC process we calculate the rate of $D^0 - \bar{D}^0$ mixing due to the exchange of non-zero Kaluza-Klein gluons at the tree level. Flavor mixing is argued to be realized by the fact that the bulk mass term and brane localized mass term is not diagonalized simultaneously unless bulk masses are degenerate. It is shown that automatic suppression mechanism is operative for the FCNC processes of light quarks. We therefore obtain a lower bound on the compactification scale of order $\mathcal{O}(\text{TeV})$ by comparing our prediction on the mass difference of neutral D meson with the recent experimental data, which is much milder than what we naively expect assuming only the decoupling of non-zero Kaluza-Klein gluons.

¹ Present address: Department of Physics, and Research and Education Center for Natural Sciences, Keio University, Hiyoshi, Yokohama, 223-8521 Japan.

1 Introduction

The origin of electroweak gauge symmetry breaking is still mysterious in particle physics. Though in the Standard Model (SM), Higgs boson is assumed to play a role for the symmetry breaking, it seems to have various theoretical problems such as the hierarchy problem and the presence of many theoretically unpredicted arbitrary coupling constants in its interactions.

Gauge-Higgs unification (GHU) [1] is one of the attractive scenarios to go beyond the standard model. It provides a possible solution to the hierarchy problem without invoking supersymmetry, also shedding some light on the long standing arbitrariness problem of Higgs interactions. In this scenario, Higgs boson in the SM is identified with the extra spatial components of the higher dimensional gauge fields. Remarkable feature is that the quantum correction to Higgs mass is UV-finite and calculable without invoking supersymmetry regardless of the non-renormalizability of higher dimensional gauge theory. This feature is guaranteed by the higher dimensional gauge invariance and has opened up a new avenue to the solution to the hierarchy problem [2]. The finiteness of the Higgs mass has been studied and verified in various models and types of compactification at one-loop level² [3] and even at the two loop level [5]. The fact that the Higgs boson is a part of gauge fields implies that Higgs interactions are restricted by gauge principle and may provide a possibility to solve the arbitrariness problem of Higgs interactions.

From such point of view, it seems that for the GHU to be phenomenologically viable, the following issues have special importance.

- (1) Are there any characteristic and generic predictions on the observables, which are subject to precision tests ?
- (2) How are the flavor structure of fermion masses and flavor mixings realized in the Yukawa couplings starting from higher dimensional gauge interaction ?
- (3) In view of the fact that Higgs interactions are basically gauge interactions with real gauge coupling constants, how is CP violated ?

As for the issue (1), it will be desirable to find finite (UV-insensitive) and calculable observables, in spite of the fact that the theory is non-renormalizable and observables are very UV-sensitive in general. Works on the oblique electroweak parameters and fermion anomalous magnetic moment from such a viewpoint already have been done in the literature [6]-[8]. The issue (3) has been addressed in our previous papers [9], [10], where CP violation is claimed to be achieved “spontaneously” either by the VEV of the Higgs field or by the “complex structure” of the compactified extra space.

In this paper, we focus on the remaining issue (2) concerning the flavor physics in the GHU scenario. It is highly non-trivial problem to explain the variety of fermion masses and flavor mixings in this scenario, since the gauge interactions should be universal

²For the case of gravity-gauge-Higgs unification, see [4].

for all matter fields, while the flavor symmetry has to be broken eventually in order to distinguish each flavor and to realize their mixings. In our previous paper [11], we addressed this issue and have clarified the mechanism to generate the flavor mixings by the interplay between bulk masses and the brane localized masses. As a remarkable property of higher dimensional gauge theories gauge invariant bulk mass terms are allowed in the form of sign functions of the extra space coordinate y . In the SM $SU(2)$ left-handed doublet of fermions couples to both of up-type and down-type right-handed fermions simultaneously. In the GHU, however, the up- and down-type right-handed fermions belong to different representations of gauge group, in general. Thus they couple to two independent left-handed doublets to form Yukawa couplings and therefore it is needed to introduce brane-localized fermions such that they form brane-localized mass terms with some linear combinations of the doublets in order to eliminate the redundant degrees of freedom.

Important point is that such introduced two types of mass terms generically may be flavor non-diagonal without contradicting with gauge invariance. This property then leads to the flavor mixing in the up- and down-types of Yukawa couplings [13]. We may start with the base where the bulk mass terms are diagonalized, since the bulk mass terms are written in the form of hermitian matrix, which may be diagonalized by suitable unitary transformations, keeping the kinetic and gauge interaction terms of fermions invariant [11]. Even in this base, however, the brane-localized mass terms still have off-diagonal elements in the flavor base in general. Namely, the fact that in general two types of fermion mass terms cannot be diagonalized simultaneously leads to physical flavor mixing. This is why we stress that the interplay between these two types of mass terms is crucial.

At first thought, one might think that only the brane localized mass terms are enough to generate the flavor mixings since they can be put by hand. However, it is not the case. We have shown that the flavor mixings disappear in the limit of universal bulk masses where the hierarchy of fermion masses is absent [11]. The reason is in this limit the bulk mass terms remain flavor-diagonal for arbitrary unitary transformation of each representation of bulk fermions. By use of this degree of freedom the Yukawa couplings are readily made diagonal. This is a remarkable feature of the GHU scenario, which is not shared by, e.g., the universal extra dimension where the flavor mixing may be caused by Yukawa couplings in the bulk just as in the standard model.

Once the flavor mixings are realized, it will be important to discuss flavor changing neutral current (FCNC) processes, which have been playing a crucial role for checking the viability of various new physics models, as is seen in the case of SUSY model. This issue was first discussed in [14] in the context of extra dimensions. Since our model reduces to the SM at low energies, there is no FCNC processes at the tree level with respect to the zero mode fields. It, however, turns out that the exchange of non-zero Kaluza-Klein (KK) modes of gauge bosons causes FCNC at the tree level, though the rates of FCNC

are suppressed by the inverse powers of the compactification scale (“decoupling”) [11]. The reason is the following.

As a genuine feature of the higher dimensional gauge theories with orbifold compactification, the gauge invariant bulk mass terms for fermions, generically written as $M\epsilon(y)\bar{\psi}\psi$ with $\epsilon(y)$ being the sign function of extra space coordinate y , are allowed. The bulk mass M may be different depending on each generation and can be an important new source of the flavor violation. The presence of the mass terms causes the localization of Weyl fermions in two different fixed points of the orbifold depending on their chiralities and the Yukawa coupling obtained by the overlap integral over y of the mode functions of Weyl fermions with different chiralities is suppressed by a factor $2\pi RMe^{-\pi RM}$ (R : the size of the extra space), which is otherwise just gauge coupling g and universal for all flavors. Thus in GHU scenario, fermion masses are all equal and of weak scale M_W to start with and the observed hierarchical small fermion masses can be achieved without fine tuning thanks to the exponential suppression factor $e^{-\pi RM}$. On the other hand, this means that the criteria by Glashow-Weinberg [15] in 4D space-time is not enough to ensure natural flavor conservation. Namely, the gauge couplings of non-zero KK modes of gauge boson, whose mode functions are y -dependent, are no longer universal even for Weyl fermions with definite chirality and the same quantum numbers, since the overlap integral of mode function of fermion and KK gauge boson depends on the bulk mass M . Thus once we move to the base of mass-eigenstates FCNC appears at the tree level.

In the previous paper, as a typical process of FCNC, we calculated the $K^0 - \bar{K}^0$ mixing amplitude at the tree level via non-zero KK gluon exchange and obtained the lower bounds for the compactification scale as the predictions of our model [11].³ Interestingly, the obtained lower bound of $\mathcal{O}(10)$ TeV was much milder than we naively expect assuming that the amplitude is simply suppressed by the inverse powers of the compactification scale, say $\mathcal{O}(10^3)$ TeV. We pointed out the presence of suppression mechanism of the FCNC process, operative for light fermions in the GHU model. As was mentioned above, fermion masses much smaller than M_W are realized by the localizations of fermions. Larger the bulk mass M , the localization of fermion is steeper and therefore for the fermions the mode functions of KK gluons seem to be almost constant. Thus for light fermions the gauge couplings of KK gluons become almost universal, just as in the case of the zero-mode sector.

In the analysis, our mechanisms of the flavor mixing and the suppression of FCNC were applied to the down-type quark sector, but the mechanisms should be also applicable to the up-type quark sector. In this paper, we turn to the $D^0 - \bar{D}^0$ mixing, which is caused

³Constraints from $K^0 - \bar{K}^0$ mixing have been discussed in [12] for a similar model as ours although it is not the gauge-Higgs unification. Similar suppression mechanism of FCNC for light quarks to the one discussed in this paper has been pointed out to be operative in this reference.

by the mixing between up and charm quarks. The $D^0 - \bar{D}^0$ mixing is not only the typical FCNC process in up-type quark sector, but also plays special role in exploring physics beyond the SM. Namely, in the SM the $\Delta C = 2$ FCNC process is realized through “box diagram” where internal quarks are of down-type, though in addition to such “short distance” contribution poorly known “long distance” contribution due to non-perturbative QCD effects are claimed to be important. The mass-squared differences of down-type quarks are much smaller than those of up-type quarks. Thus the expected contribution to the mass difference of neutral D meson $\Delta M_D(\text{SD})$ due to $D^0 - \bar{D}^0$ mixing is expected to be small in the SM:

$$x_D(\text{SM}) = \frac{\Delta M_D(\text{SM})}{\Gamma_D} \lesssim 10^{-3}, \quad (1.1)$$

where Γ_D is the decay width of neutral D meson. Hence if the $D^0 - \bar{D}^0$ mixing and/or associated CP violating observable with relatively large rates are found it suggests the presence of some new physics. As the matter of fact, recently impressive progress has been made by BABAR and Belle in the measurement [16]:

$$x_D(\text{exp}) = (1.00 \pm 0.25) \times 10^{-2}. \quad (1.2)$$

We will calculate the dominant contribution to the process at the tree level by the exchange of non-zero KK gluons. Comparing the obtained finite contribution to the mixing with the allowed range for the new physics contribution derived from the experimental data, we put the lower bound on the compactification scale. It will be also discussed how the extent of the suppression of FCNC process is different depending on the type of contributing effective 4-Fermi operators, i.e. the operators made by the product of currents with the same chirality (LL and RR type) and different chiralities (LR type).

This paper is organized as follows. After introducing our model in the next section, we summarize in section 3 how the flavor mixing is realized in the context of the gauge-Higgs unification, which was clarified and described in detail in our previous paper [11]. In section 4, as an application of the flavor mixing discussed in section 3, we calculate the mass difference of neutral D -mesons caused by the $D^0 - \bar{D}^0$ mixing via non-zero KK gluon exchange at the tree level. We also obtain the lower bound for the compactification scale by comparing the obtained result with the experimental data. The origin of the suppression mechanism of FCNC process is discussed in section 5, emphasizing the importance of the localization of quark fields and the fact that FCNC is controlled by the non-degeneracy of bulk masses, which is specific to the gauge-Higgs unification. Also discussed is the origin of the different extent of the suppression depending on the chirality of the relevant 4-Fermi operator. Section 6 is devoted to our conclusions. The results of more careful and thorough study of $K^0 - \bar{K}^0$ mixing taking into account the contributions of the operators of LL and RR types, which was not carried out in our previous paper [11], are briefly given in Appendix A.

2 The Model

Although the model we consider in this paper is the same as the one taken in [11], we briefly describe the model for completeness. The model taken in this paper is a five dimensional (5D) $SU(3) \otimes SU(3)_{\text{color}}$ GHU model compactified on an orbifold S^1/Z_2 with a radius R of S^1 . As matter fields, we introduce n generations of bulk fermion in the $\mathbf{3}$ and the $\bar{\mathbf{6}}$ dimensional representations of $SU(3)$ gauge group denoted by a column vector and a 3×3 matrix, $\psi^i(\mathbf{3})$ and $\psi^i(\bar{\mathbf{6}})$ ($i = 1, \dots, n$) [13].

The bulk Lagrangian is given by

$$\begin{aligned} \mathcal{L} = & -\frac{1}{2}\text{Tr}(F_{MN}F^{MN}) - \frac{1}{2}\text{Tr}(G_{MN}G^{MN}) \\ & + \bar{\psi}^i(\mathbf{3})\{i\not{D}_3 - M^i\epsilon(y)\}\psi^i(\mathbf{3}) + \frac{1}{2}\text{Tr}\left[\bar{\psi}^i(\bar{\mathbf{6}})\{i\not{D}_6 - M^i\epsilon(y)\}\psi^i(\bar{\mathbf{6}})\right] \end{aligned} \quad (2.1)$$

where

$$F_{MN} = \partial_M A_N - \partial_N A_M - ig[A_M, A_N], \quad (2.2)$$

$$G_{MN} = \partial_M G_N - \partial_N G_M - ig_s[G_M, G_N], \quad (2.3)$$

$$\not{D}_3\psi^i(\mathbf{3}) = \Gamma^M(\partial_M - igA_M - ig_sG_M)\psi^i(\mathbf{3}), \quad (2.4)$$

$$\not{D}_6\psi^i(\bar{\mathbf{6}}) = \Gamma^M\left[\partial_M\psi^i(\bar{\mathbf{6}}) + ig\{A_M^*\psi^i(\bar{\mathbf{6}}) + \psi^i(\bar{\mathbf{6}})(A_M)^\dagger\} - ig_sG_M\psi^i(\bar{\mathbf{6}})\right], \quad (2.5)$$

with G_M being understood to act on the color index, not explicitly written here. The gauge fields A_M and G_M are written in a matrix form, e.g. $A_M = A_M^a \frac{\lambda^a}{2}$ in terms of Gell-Mann matrices λ^a . $M, N = 0, 1, 2, 3, 5$ and the five dimensional gamma matrices are given by $\Gamma^M = (\gamma^\mu, i\gamma^5)$ ($\mu = 0, 1, 2, 3$). g and g_s are 5D gauge coupling constants of $SU(3)$ and $SU(3)_{\text{color}}$, respectively. M^i are generation dependent bulk mass parameters of the fermions accompanied by the sign function $\epsilon(y)$. As was discussed in the introduction, here we take the base where the bulk mass term is flavor-diagonal.

The periodic boundary condition is imposed along S^1 and Z_2 parity assignments are taken for gauge fields as

$$\begin{aligned} A_\mu = & \begin{bmatrix} (+,+) & (+,+) & (-,-) \\ (+,+) & (+,+) & (-,-) \\ (-,-) & (-,-) & (+,+) \end{bmatrix}, \quad A_y = \begin{bmatrix} (-,-) & (-,-) & (+,+) \\ (-,-) & (-,-) & (+,+) \\ (+,+) & (+,+) & (-,-) \end{bmatrix}, \\ G_\mu = & \begin{bmatrix} (+,+) & (+,+) & (+,+) \\ (+,+) & (+,+) & (+,+) \\ (+,+) & (+,+) & (+,+) \end{bmatrix}, \quad G_y = \begin{bmatrix} (-,-) & (-,-) & (-,-) \\ (-,-) & (-,-) & (-,-) \\ (-,-) & (-,-) & (-,-) \end{bmatrix}, \end{aligned} \quad (2.6)$$

where $(+,+)$ etc. stand for Z_2 parities at fixed points $y = 0, \pi R$. We can see that the gauge symmetry is explicitly broken as $SU(3) \rightarrow SU(2) \times U(1)$ by the boundary conditions. The gauge fields with Z_2 parities $(+,+)$ and $(-,-)$ are mode-expanded by use of mode functions, which are just trigonometric functions, i.e. $S_n(y) = \frac{1}{\sqrt{\pi R}} \sin(M_n y)$ and $C_n(y) = \frac{1}{\sqrt{\pi R}} \cos(M_n y)$ ($n \neq 0$), $C_0(y) = \frac{1}{\sqrt{2\pi R}}$, respectively.

The Z_2 parities of fermions are assigned for each component of the representations as follows:

$$\begin{aligned}\Psi^i(\mathbf{3}) &= (Q_{3L}^i(+, +) + Q_{3R}^i(-, -)) \oplus (d_L^i(-, -) + d_R^i(+, +)), \\ \Psi^i(\bar{\mathbf{6}}) &= (\Sigma_L^i(-, -) + \Sigma_R^i(+, +)) \oplus (Q_{6L}^i(+, +) + Q_{6R}^i(-, -)) \oplus (u_L^i(-, -) + u_R^i(+, +))\end{aligned}\quad (2.7)$$

where Q_3^i and Q_6^i are $SU(2)$ doublets and d^i and u^i are $SU(2)$ singlets. $\psi^i(\bar{\mathbf{6}})$ also contain $SU(2)$ triplet exotic states Σ^i written in a form of 2×2 symmetric matrix [13]. In this way a chiral theory is realized in the zero mode sector by Z_2 orbifolding.

The fermions are also expanded by an ortho-normal set of mode functions. Here we will focus on the zero-mode sector, which are necessary for the argument of flavor mixing:

$$\psi^i(\mathbf{3}) = \begin{bmatrix} Q_{3L}^i f_L^i(y) \\ d_R^i f_R^i(y) \end{bmatrix}, \quad (2.8)$$

$$\psi^i(\bar{\mathbf{6}}) = \left[\begin{array}{c|c} (i\sigma^2)\Sigma^i(i\sigma^2)^T & \frac{1}{\sqrt{2}}(i\sigma^2)Q_6^i \\ \hline \frac{1}{\sqrt{2}}(Q_6^i)^T(i\sigma^2)^T & u^i \end{array} \right] \quad (2.9)$$

where $i\sigma^2$ denotes an $SU(2)$ invariant anti-symmetric tensor $(i\sigma^2)^{\alpha\beta} = \epsilon^{\alpha\beta}$. The zero mode sector of each component of $\psi^i(\bar{\mathbf{6}})$ is written in terms of the same mode functions as in the case of $\psi^i(\mathbf{3})$.

$$\Sigma^i = \Sigma_R^i f_R^i(y), \quad Q_6^i = Q_{6L}^i f_L^i(y), \quad u^i = u_R^i f_R^i(y). \quad (2.10)$$

The mode function for the zero mode of each chirality is given in [9]:

$$f_L^i(y) = \sqrt{\frac{M^i}{1 - e^{-2\pi R M^i}}} e^{-M^i|y|}, \quad f_R^i(y) = \sqrt{\frac{M^i}{e^{2\pi R M^i} - 1}} e^{M^i|y|}. \quad (2.11)$$

We notice that there are two left-handed quark doublets Q_{3L} and Q_{6L} per generation in the zero mode sector, which are massless before electro-weak symmetry breaking. In the one generation case, for instance, one of two independent linear combinations of these doublets should correspond to the quark doublet in the standard model, but the other one should be regarded as an exotic state. Moreover, we have an exotic fermion Σ_R . We therefore introduce brane localized four dimensional Weyl spinors to form $SU(2) \times U(1)$ invariant brane localized Dirac mass terms in order to remove these exotic massless fermions from the low-energy effective theory [13, 17].

$$\begin{aligned}\mathcal{L}_{\text{BM}} &= \int_{-\pi R}^{\pi R} dy \sqrt{2\pi R} \delta(y) \bar{Q}_R^i(x) \left\{ \eta_{ij} Q_{3L}^j(x, y) + \lambda_{ij} Q_{6L}^j(x, y) \right\} \\ &\quad + \int_{-\pi R}^{\pi R} dy \sqrt{2\pi R} m_{\text{BM}} \delta(y - \pi R) \text{Tr} \left\{ \bar{\Sigma}_R^i(x, y) \chi_L^i(x) \right\} + (\text{h.c.})\end{aligned}\quad (2.12)$$

where Q_R and χ_L are the brane localized Weyl fermions of doublet and the triplet of $SU(2)$ respectively. The $n \times n$ matrices η_{ij} , λ_{ij} and m_{BM} are mass parameters. These

brane localized mass terms are introduced at opposite fixed points such that $Q_R(\chi_L)$ couples to $Q_{3,6L}(\Sigma_R)$ localized on the brane at $y = 0$ ($y = \pi R$). Let us note that the matrices η_{ij}, λ_{ij} can be non-diagonal, which causes the flavor mixing [11] [13].

Some comments on this model are in order. The predicted Weinberg angle of this model is not realistic, $\sin^2 \theta_W = 3/4$. Possible modification is to introduce an extra $U(1)$ or the brane localized gauge kinetic term [18]. However, the wrong Weinberg angle does not affect our argument, since our interest is $D^0 - \bar{D}^0$ mixing via KK gluon exchange in the QCD sector, whose amplitude is independent of the Weinberg angle.

Second, in our model the bulk masses of fermions are generation-dependent, but are taken as common for both $\psi^i(\mathbf{3})$ and $\psi^i(\bar{\mathbf{6}})$. In general, the bulk masses of each representation are mutually independent and there is no physical reason to take such a choice. It would be justified if we have some Grand Unified Theory (GUT) where the $\mathbf{3}$ and $\bar{\mathbf{6}}$ representations are embedded into a single multiplet of the GUT gauge group. We do not further pursue this issue in this paper.

3 Flavor mixing

In the previous section we worked in the base where fermion bulk mass terms are written in a diagonal matrix in the generation space. Then the lagrangian for fermions, which includes Yukawa couplings as the gauge interaction of A_y is completely diagonalized in the generation space. Thus flavor mixing does not occur in the bulk and the brane localized mass terms for the doubled doublets Q_{3L} and Q_{6L} is expected to lead to the flavor mixing. We now confirm the expectation and discuss how the flavor mixing is realized in this model.

First, we identify the SM quark doublet by diagonalizing the relevant brane localized mass term,

$$\begin{aligned} \int_{-\pi R}^{\pi R} dy \sqrt{2\pi R} \delta(y) \bar{Q}_R(x) \begin{bmatrix} \eta & \lambda \end{bmatrix} \begin{bmatrix} Q_{3L}(x, y) \\ Q_{6L}(x, y) \end{bmatrix} &\supset \sqrt{2\pi R} \bar{Q}_R(x) \begin{bmatrix} \eta f_L(0) & \lambda f_L(0) \end{bmatrix} \begin{bmatrix} Q_{3L}(x) \\ Q_{6L}(x) \end{bmatrix} \\ &= \sqrt{2\pi R} \bar{Q}'_R(x) \begin{bmatrix} m_{\text{diag}} & \mathbf{0}_{n \times n} \end{bmatrix} \begin{bmatrix} Q_{\text{HL}}(x) \\ Q_{\text{SML}}(x) \end{bmatrix} \end{aligned} \quad (3.1)$$

where

$$\begin{bmatrix} U_1 & U_3 \\ U_2 & U_4 \end{bmatrix} \begin{bmatrix} Q_{\text{HL}}(x) \\ Q_{\text{SML}}(x) \end{bmatrix} = \begin{bmatrix} Q_{3L}(x) \\ Q_{6L}(x) \end{bmatrix}, \quad U^{\bar{Q}} Q_R(x) = Q'_R(x), \quad (3.2)$$

$$U^{\bar{Q}} \begin{bmatrix} \eta f_L(0) & \lambda f_L(0) \end{bmatrix} \begin{bmatrix} U_1 & U_3 \\ U_2 & U_4 \end{bmatrix} = \begin{bmatrix} m_{\text{diag}} & \mathbf{0}_{n \times n} \end{bmatrix}. \quad (3.3)$$

In eq. (3.1), $\eta f_L(0)$ is an abbreviation of a $n \times n$ matrix whose (i, j) element is given by $\eta_{ij} f_L^j(0)$, for instance. U_3, U_4 are $n \times n$ matrices which indicate how the quark doublets

of the SM are contained in each of $Q_{3L}(x)$ and $Q_{6L}(x)$ and compose a $2n \times 2n$ unitary matrix together with U_1 , U_2 , which diagonalizes the brane localized mass matrix. The eigenstate Q_H becomes massive and decouples from the low energy processes, while Q_{SM} remains massless at this stage and therefore is identified with the SM quark doublet. U_3 and U_4 satisfy the following unitarity condition:

$$U_3^\dagger U_3 + U_4^\dagger U_4 = \mathbf{1}_{n \times n}. \quad (3.4)$$

After this identification of the SM doublet, Yukawa couplings are read off from the higher dimensional gauge interaction of A_y , whose zero mode is the Higgs field $H(x)$:

$$\begin{aligned} & \int_{-\pi R}^{\pi R} dy \left[-\frac{g}{2} \bar{\psi}^i(\mathbf{3}) A_y^a \lambda^a \Gamma^y \psi^i(\mathbf{3}) + g \text{Tr} \left\{ \bar{\psi}^i(\bar{\mathbf{6}}) A_y^a (\lambda^a)^* \Gamma^y \psi^i(\bar{\mathbf{6}}) \right\} \right] \\ & \supset \int_{-\pi R}^{\pi R} dy \left\{ -g \bar{Q}_{3L}^i(x, y) H(x, y) d_R^i(x, y) - \sqrt{2} g \bar{Q}_{6L}^i(x, y) i\sigma^2 H^*(x, y) u_R^i(x, y) + (\text{h.c.}) \right\} \\ & \supset -g_4 \left[\langle H^\dagger \rangle \bar{d}_R^i(x) I_{RL}^{i(00)} U_3^{ij} Q_{SML}^j(x) + \sqrt{2} \langle H^\dagger \rangle i\sigma^2 \bar{u}_R^i(x) I_{RL}^{i(00)} U_4^{ij} Q_{SML}^j(x) \right] + (\text{h.c.}) \end{aligned} \quad (3.5)$$

where $g_4 \equiv \frac{g}{\sqrt{2\pi R}}$ and

$$I_{RL}^{i(00)} = \int_{-\pi R}^{\pi R} dy f_L^i f_R^i = \frac{\pi R M^i}{\sinh(\pi R M^i)}, \quad (3.6)$$

which behaves as $2\pi R M^i e^{-\pi R M^i}$ for $\pi R M^i \gg 1$, thus realizing the hierarchical small quark masses without fine tuning of M^i . We thus know that the matrices of Yukawa coupling $g_4 Y_u$ and $g_4 Y_d$ are given as

$$g_4 Y_u = \sqrt{2} g_4 I_{RL}^{(00)} U_4, \quad g_4 Y_d = g_4 I_{RL}^{(00)} U_3, \quad (3.7)$$

where the matrix $I_{RL}^{(00)}$ has elements $(I_{RL}^{(00)})_{ij} = \delta_{ij} I_{RL}^{i(00)}$. These matrices are diagonalized by bi-unitary transformations as in the SM and Cabibbo-Kobayashi-Maskawa matrix is defined in a usual way.

$$\begin{cases} \hat{Y}_d = \text{diag}(\hat{m}_d, \dots) = V_{dR}^\dagger Y_d V_{dL} \\ \hat{Y}_u = \text{diag}(\hat{m}_u, \dots) = V_{uR}^\dagger Y_u V_{uL} \end{cases}, \quad V_{CKM} \equiv V_{dL}^\dagger V_{uL} \quad (3.8)$$

where all the quark masses are normalized by the W -boson mass as $\hat{m}_f = \frac{m_f}{M_W}$. A remarkable point is that the Yukawa couplings $g_4 Y_u$ and $g_4 Y_d$ are mutually related by the unitarity condition eq. (3.4), on the contrary those are completely independent in the Standard Model. Thus if we set bulk masses of fermion to be universal among generations, i.e. $M^1 = M^2 = M^3 = \dots = M^n$, then $I_{RL}^{(00)}$ is proportional to the unit matrix. In such a case, $Y_u^\dagger Y_u \propto U_4^\dagger U_4$ and $Y_d^\dagger Y_d \propto U_3^\dagger U_3$ can be simultaneously diagonalized because of the unitarity condition eq. (3.4). This means that the flavor mixing disappears in the limit of universal bulk masses, as was expected in the introduction. In reality, off course the bulk

masses should be different to explain the variety of quark masses and therefore the flavor mixing does not vanish.

For an illustrative purpose to confirm the mechanism of flavor mixing, let us consider the two generation case. We will see how the realistic quark masses and mixing are reproduced. For simplicity, we ignore CP violation and assume that U_3, U_4 are real. Let us notice that from the unitarity condition shown in (3.4), $U_3^\dagger U_3 + U_4^\dagger U_4 = \mathbf{1}_{2 \times 2}$, 2×2 matrices $U_{3,4}$ can be parametrized without loss of generality as

$$U_4 = \begin{bmatrix} \cos \theta' & -\sin \theta' \\ \sin \theta' & \cos \theta' \end{bmatrix} \begin{bmatrix} a & 0 \\ 0 & b \end{bmatrix}, \quad U_3 = \begin{bmatrix} \cos \theta & -\sin \theta \\ \sin \theta & \cos \theta \end{bmatrix} \begin{bmatrix} \sqrt{1-a^2} & 0 \\ 0 & \sqrt{1-b^2} \end{bmatrix}. \quad (3.9)$$

Actually the most general forms of U_3 and U_4 have a common orthogonal matrix multiplied from the right, being consistent with (3.4). The common orthogonal matrix, however, can be eliminated by suitable unitary transformation among the members of $Q_{\text{SML}}(x)$.

Let us note that if we wish, instead of the base where bulk mass term is diagonalized, we can move to another base where $\theta = \theta' = 0$ by suitable unitary transformations of Q_3 and Q_6 . Then in this base the bulk mass term is no longer diagonal in the generation space unless bulk masses are degenerate, and the off-diagonal elements lead to flavor mixing. In the specific case of degenerate bulk masses, the bulk mass term is still diagonal and flavor mixing disappears. This is another proof of why flavor mixing disappears for degenerate bulk masses.

The integral $I_{RL}^{(00)}$ is parametrized as follows.

$$I_{RL}^{(00)} = \begin{bmatrix} c & 0 \\ 0 & d \end{bmatrix}. \quad (3.10)$$

Now physical observables $\hat{m}_u, \hat{m}_c, \hat{m}_d, \hat{m}_s$ and the Cabibbo angle θ_c are all written in terms of a, b, c, d and θ, θ' . Namely trivial relations

$$\det(\hat{Y}_d^\dagger \hat{Y}_d) = \hat{m}_d^2 \hat{m}_s^2, \quad \det(\hat{Y}_u^\dagger \hat{Y}_u) = \hat{m}_u^2 \hat{m}_c^2, \quad (3.11)$$

$$\text{Tr}(\hat{Y}_d^\dagger \hat{Y}_d) = \hat{m}_d^2 + \hat{m}_s^2, \quad \text{Tr}(\hat{Y}_u^\dagger \hat{Y}_u) = \hat{m}_u^2 + \hat{m}_c^2 \quad (3.12)$$

provide through eqs. (3.7)-(3.10) with

$$\hat{m}_d^2 \hat{m}_s^2 = (1-a^2)(1-b^2)c^2 d^2, \quad (3.13)$$

$$\hat{m}_d^2 + \hat{m}_s^2 = (1-a^2)c^2 + (1-b^2)d^2 + (a^2-b^2)(c^2-d^2)\sin^2 \theta, \quad (3.14)$$

$$\hat{m}_u^2 \hat{m}_c^2 = 4a^2 b^2 c^2 d^2, \quad (3.15)$$

$$\hat{m}_u^2 + \hat{m}_c^2 = 2 \left\{ a^2 c^2 + b^2 d^2 - (a^2 - b^2)(c^2 - d^2) \sin^2 \theta' \right\}. \quad (3.16)$$

We also note that θ_c is given as

$$\tan 2\theta_c = \frac{\tan 2\theta_{dL} - \tan 2\theta_{uL}}{1 + \tan 2\theta_{dL} \tan 2\theta_{uL}}, \quad (3.17)$$

$$\tan 2\theta_{dL} = \frac{2\sqrt{(1-a^2)(1-b^2)}(d^2 - c^2) \sin \theta \cos \theta}{(1-a^2)(c^2 \cos^2 \theta + d^2 \sin^2 \theta) - (1-b^2)(c^2 \sin^2 \theta + d^2 \cos^2 \theta)} , \quad (3.18)$$

$$\tan 2\theta_{uL} = \frac{2ab(d^2 - c^2) \sin \theta' \cos \theta'}{a^2(c^2 \cos^2 \theta' + d^2 \sin^2 \theta') - b^2(c^2 \sin^2 \theta' + d^2 \cos^2 \theta')} \quad (3.19)$$

where angles θ_{dL} , θ_{uL} are angles parametrizing V_{dL} , V_{uL} , respectively. Note that five physical observables are written in terms of six parameters, a, b, c, d and θ, θ' . So our theory has one degree of freedom which cannot be determined by the observables. We choose θ' as a free parameter. Then once we choose the value of θ' , other 5 parameters can be completely fixed by the observables, by solving eqs. (3.13)-(3.19) numerically for a, b, c, d and θ . The result is shown in Table 1.⁴

$\sin \theta'$	a^2	b^2	c^2	d^2	$\sin \theta$
-0.9999	0.000015	0.999998	3.94×10^{-9}	1	-0.00016
-0.8	0.0463	0.9951	4.07×10^{-9}	3.22×10^{-4}	-0.00383
-0.6	0.0770	0.9916	4.19×10^{-9}	1.88×10^{-4}	0.00195
-0.4	0.0959	0.9894	4.31×10^{-9}	1.47×10^{-4}	0.00992
-0.2	0.1052	0.9882	4.43×10^{-9}	1.31×10^{-4}	0.01845
0.0	0.1062	0.9881	4.55×10^{-9}	1.26×10^{-4}	0.02649
0.2	0.0997	0.9889	4.68×10^{-9}	1.31×10^{-4}	0.03315
0.4	0.0860	0.9906	4.80×10^{-9}	1.48×10^{-4}	0.03745
0.6	0.0650	0.9930	4.93×10^{-9}	1.89×10^{-4}	0.03806
0.8	0.0365	0.9962	5.07×10^{-9}	3.27×10^{-4}	0.03239
0.9999	0.000012	0.999998	5.23×10^{-9}	1	0.00064

Table 1: Numerical result for the relevant parameters fixed by quark masses and Cabibbo angle.

Thus we have confirmed that observed quark masses and flavor mixing angle can be reproduced in our model of GHU. Let us note that in eq. (3.17) Cabibbo angle θ_c vanishes in the limit of universal bulk mass, i.e. $M^1 = M^2$ leads to $c = d$ as is expected.

4 $D^0 - \bar{D}^0$ mixing

In this section, we apply the results of the previous section to a representative FCNC process, $D^0 - \bar{D}^0$ mixing responsible for the mass difference of two neutral D mesons.⁵

We focus on the FCNC processes of zero mode up-type quarks due to gauge boson exchange at the tree level. First let us consider the processes with the exchange of zero mode gauge bosons. If such type of diagrams exist with a sizable magnitude, it will easily spoil the viability of the model.

⁴ Note that $\sin \theta'$ has the upper and lower limits. As $\sin \theta'$ goes to ± 1 , the bulk mass of the second generation M^2 goes to 0 (i.e. $d = 1$). When $\sin \theta'$ takes a value beyond these limits, we have no solution.

⁵For the studies of $D^0 - \bar{D}^0$ mixing in other new physics models, see for instance [19] [20].

Concerning the Z -boson exchange, it is in principle possible to occur the tree-level FCNC. Since the mode function of the zero mode gauge boson is y -independent, the overlap integral of mode functions is universal, i.e. generation independent, just as the kinetic term of fermions are. Thus the gauge coupling of zero mode gauge boson depends on only the relevant quantum numbers such as the third component of weak isospin I_3 . Therefore the condition proposed by Glashow-Weinberg [15] to guarantee natural flavor conservation for the theories of 4D space-time is relevant. Note that we have two right-handed up-type quarks belonging to $\psi(\bar{\mathbf{6}})$, $SU(2)$ singlet u^i and a member of $SU(2)$ triplet Σ^i in (2.9). They have different I_3 , i.e. 0 and 1, while they have the same electric charge and chirality. Thus, the condition of Glashow-Weinberg is not satisfied in the up-type quark sector and FCNC process due to the exchange of the zero mode Z -boson arises at the tree level.⁶ However, the triplet Σ^i is an exotic fermion and acquires large $SU(2)$ invariant brane mass. Thus the mixing between u^i and Σ^i is inversely suppressed by the power of m_{BM} and the FCNC vertex of Z -boson can be safely neglected. We may say that the condition of Glashow-Weinberg is satisfied in a good approximation in the processes via the zero mode gauge boson exchange. Furthermore, the contribution by the weak gauge boson exchange is expected to be small compared with that by the gluon exchange.

Hence, the remaining possibility is the process via the exchange of non-zero KK gauge bosons. In this case, the mode functions of KK gauge bosons are y -dependent and their couplings to fermions are no longer universal because of non-degenerate bulk masses, even if the condition of Glashow-Weinberg is met.

Therefore, such progresses lead to FCNC at the tree level. In our previous paper [11], we have calculated $K^0 - \bar{K}^0$ mixing via the non-zero KK gluon exchange at the tree level and obtained a lower bound of the compactification scale as the prediction of our model.

Along the same line of the argument as in our previous paper, we here study $D^0 - \bar{D}^0$ mixing in the up-type quark sector caused by the non-zero KK gluon exchange at the tree level as the dominant contribution to this FCNC process.

For such purpose, we derive the four dimensional effective strong interaction vertices with respect to the zero modes of up-type quarks relevant for our calculation:

$$\begin{aligned}
\mathcal{L}_s \supset & \frac{g_s}{2\sqrt{2\pi R}} G_\mu^a \left(\bar{u}_R^i \gamma^\mu \lambda^a u_R^i + \bar{Q}_{3L}^i \lambda^a \gamma^\mu Q_{3L}^i + \bar{Q}_{6L}^i \lambda^a \gamma^\mu Q_{6L}^i \right) \\
& + \frac{g_s}{2} G_\mu^{a(n)} \left\{ \bar{u}_R^i \lambda^a \gamma^\mu u_R^i I_{RR}^{i(0n0)} + (-1)^n (\bar{Q}_{3L}^i \lambda^a \gamma^\mu Q_{3L}^i + \bar{Q}_{6L}^i \lambda^a \gamma^\mu Q_{6L}^i) I_{RR}^{i(0n0)} \right\} \\
\supset & \frac{g_s}{2\sqrt{2\pi R}} G_\mu^a \left(\bar{\tilde{u}}_R^i \gamma^\mu \lambda^a \tilde{u}_R^i + \bar{\tilde{u}}_L^i \lambda^a \gamma^\mu \tilde{u}_L^i \right) \\
& + \frac{g_s}{2} G_\mu^{a(n)} \bar{\tilde{u}}_R^i \lambda^a \gamma^\mu \tilde{u}_R^j \left(V_{uR}^\dagger I_{RR}^{(0n0)} V_{uR} \right)_{ij} \\
& + \frac{g_s}{2} G_\mu^{a(n)} \bar{\tilde{u}}_L^i \lambda^a \gamma^\mu \tilde{u}_L^j (-1)^n \left(V_{uL}^\dagger U_3^\dagger I_{RR}^{(0n0)} U_3 V_{uL} + V_{uL}^\dagger U_4^\dagger I_{RR}^{(0n0)} U_4 V_{uL} \right)_{ij} \quad (4.1)
\end{aligned}$$

⁶ The FCNC due to the exchanges of zero mode photon and gluon trivially vanish because the fermions of our interest have the same electric charge and color.

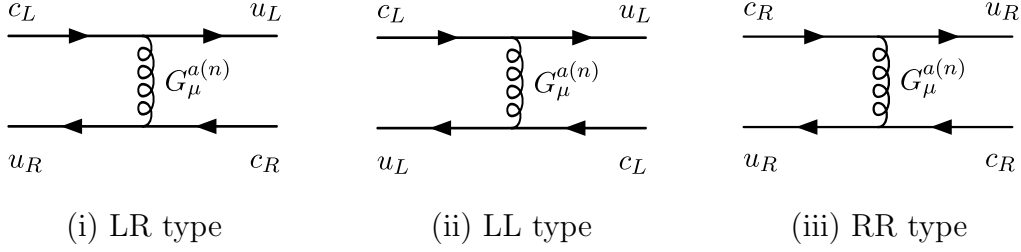


Figure 1: The diagrams of $D^0 - \bar{D}^0$ mixing via KK gluon exchange

listed above,

$$\begin{aligned}
 & \text{Diagram (i) LR type} \sim \sum_{n=1}^{\infty} \frac{g_s^2}{4} \frac{(-1)^n}{M_n^2} \left(V_{uL}^\dagger U_3^\dagger I_{RR}^{(0n0)} U_3 V_{uL} + V_{uL}^\dagger U_4^\dagger I_{RR}^{(0n0)} U_4 V_{uL} \right)_{21} \\
 & \quad \times \left(V_{uR}^\dagger I_{RR}^{(0n0)} V_{uR} \right)_{21} (\bar{u}_L \lambda^a \gamma^\mu c_L) (\bar{u}_R \lambda^a \gamma_\mu c_R). \quad (4.6)
 \end{aligned}$$

Similarly, the LL and the RR type diagrams of Fig. 1 give

$$\begin{aligned}
 & \text{Diagram (ii) LL type} \sim - \sum_{n=1}^{\infty} \frac{g_s^2}{4} \frac{1}{M_n^2} \left(V_{uL}^\dagger U_3^\dagger I_{RR}^{(0n0)} U_3 V_{uL} + V_{uL}^\dagger U_4^\dagger I_{RR}^{(0n0)} U_4 V_{uL} \right)_{21}^2 \\
 & \quad \times (\bar{u}_L \lambda^a \gamma^\mu c_L) (\bar{u}_L \lambda^a \gamma_\mu c_L), \quad (4.7)
 \end{aligned}$$

$$\begin{aligned}
 & \text{Diagram (iii) RR type} \sim - \sum_{n=1}^{\infty} \frac{g_s^2}{4} \frac{1}{M_n^2} \left(V_{uR}^\dagger I_{RR}^{(0n0)} V_{uR} \right)_{21}^2 (\bar{u}_R \lambda^a \gamma^\mu c_R) (\bar{u}_R \lambda^a \gamma_\mu c_R). \quad (4.8)
 \end{aligned}$$

The sum over the integer n is convergent and the coefficients of the effective lagrangian (4.6)-(4.8) are suppressed by the compactification scale as $1/M_c^2$ where $M_c = R^{-1}$. We can verify, as we expect, that the coefficient vanishes in the limit of universal bulk masses $M^1 = M^2 = \dots$ by use of the unitarity condition (3.4), since $I_{RR}^{(0n0)}$ is proportional to the unit matrix in this limit;

$$\begin{aligned}
 V_{uL}^\dagger \left(U_3^\dagger I_{RR}^{(0m0)} U_3 + U_4^\dagger I_{RR}^{(0m0)} U_4 \right) V_{uL} & \xrightarrow{M^1=M^2=\dots} V_{uL}^\dagger \left(U_3^\dagger U_3 + U_4^\dagger U_4 \right) V_{uL} I_{RR}^{(0m0)} \propto \mathbf{1}_{n \times n}, \\
 V_{uR}^\dagger I_{RR}^{(0m0)} V_{uR} & \xrightarrow{M^1=M^2=\dots} V_{uR} V_{uR}^\dagger I_{RR}^{(0m0)} \propto \mathbf{1}_{n \times n}. \quad (4.9)
 \end{aligned}$$

Comparing the calculation of (4.6)-(4.8) with the experimental data, we can obtain a lower bound on the compactification scale. The most general effective Hamiltonian for $\Delta C = 2$ processes due to some “new physics” at a high scale $\Lambda_{\text{NP}} \gg M_W$ can be written as follows;

$$\mathcal{H}_{\text{eff}}^{\Delta C=2} = \frac{1}{\Lambda_{\text{NP}}^2} \left(\sum_{i=1}^5 z_i Q_i + \sum_{i=1}^3 \tilde{z}_i \tilde{Q}_i \right) \quad (4.10)$$

where

$$\begin{aligned} Q_1 &= \bar{u}_L^\alpha \gamma_\mu c_L^\alpha \bar{u}_L^\beta \gamma^\mu c_L^\beta, & Q_2 &= \bar{u}_R^\alpha c_L^\alpha \bar{u}_R^\beta c_L^\beta, & Q_3 &= \bar{u}_R^\alpha c_L^\beta \bar{u}_R^\beta c_L^\alpha, \\ Q_4 &= \bar{u}_R^\alpha c_L^\alpha \bar{u}_L^\beta c_R^\beta, & Q_5 &= \bar{u}_R^\alpha c_L^\beta \bar{u}_L^\beta c_R^\alpha, \end{aligned} \quad (4.11)$$

and indices α, β stand for the color degrees of freedom. The operators $\tilde{Q}_{1,2,3}$ are obtained from the $Q_{1,2,3}$ by the chirality exchange $L \leftrightarrow R$. Since the contribution of the SM to the mixing is poorly known, we can get the constraint on the new physics directly from the experimental data assuming that there is no accidental cancellation between the contributions of the SM and new physics. If we assume one of these possible operators gives dominant contribution to the mixing, each coefficient is independently constrained as follows, with the constraints for \tilde{z}_i are the same with those for z_i ($i = 1, 2, 3$) [19];

$$\begin{aligned} |z_1| &\leq 5.7 \times 10^{-7} \left(\frac{\Lambda_{\text{NP}}}{1\text{TeV}} \right)^2, & |z_2| &\leq 1.6 \times 10^{-7} \left(\frac{\Lambda_{\text{NP}}}{1\text{TeV}} \right)^2, \\ |z_3| &\leq 5.8 \times 10^{-7} \left(\frac{\Lambda_{\text{NP}}}{1\text{TeV}} \right)^2, & |z_4| &\leq 5.6 \times 10^{-8} \left(\frac{\Lambda_{\text{NP}}}{1\text{TeV}} \right)^2, \\ |z_5| &\leq 1.6 \times 10^{-7} \left(\frac{\Lambda_{\text{NP}}}{1\text{TeV}} \right)^2 \end{aligned} \quad (4.12)$$

where Λ_{NP} is regarded as the compactification scale in our case. All we have to do is to represent (4.6)-(4.8) by use of (4.11) and to utilize these constraints (4.12).

We can rewrite the LR type effective lagrangian (4.6) in terms of scalar type effective Hamiltonian by using the Fiertz transformation;

$$-\frac{\pi\alpha_s}{2}(\alpha_u + \alpha'_u) \sin 2\theta_{uR} R^2 S_{\text{KK}}^{LR} \left(4Q_4 - \frac{4}{3}Q_5 \right) \quad (4.13)$$

where we use a following relation about Gell-Mann matrices λ^a normalized as $\text{Tr}(\lambda^a \lambda^b) = 2\delta^{ab}$;

$$\sum_{a=1}^8 (\lambda^a)_{\alpha\beta} (\lambda^a)_{\gamma\delta} = 2\delta_{\alpha\delta} \delta_{\beta\gamma} - \frac{2}{3} \delta_{\alpha\beta} \delta_{\gamma\delta} \quad (4.14)$$

and the four-dimensional α_s is defined by

$$\alpha_s = \frac{(g_s^{4D})^2}{4\pi} = \frac{1}{2\pi R} \frac{g_s^2}{4\pi}. \quad (4.15)$$

Parameters in (4.13) are defined as follows:

$$\begin{aligned} \alpha_u &\equiv -(1 - a^2) \sin 2\theta_{uL} \cos^2 \theta + (1 - b^2) \sin 2\theta_{uL} \sin^2 \theta \\ &\quad - \sqrt{(1 - a^2)(1 - b^2)} \cos 2\theta_{uL} \sin 2\theta, \end{aligned} \quad (4.16)$$

$$\alpha'_u \equiv -a^2 \sin 2\theta_{uL} \cos^2 \theta' + b^2 \sin 2\theta_{uL} \sin^2 \theta' - ab \cos 2\theta_{uL} \sin 2\theta', \quad (4.17)$$

$$S_{\text{KK}}^{LR} \equiv \pi R \sum_{n=1}^{\infty} \frac{(-1)^n}{n^2} \left(I_{RR}^{1(0n0)} - I_{RR}^{2(0n0)} \right)^2 \quad (4.18)$$

and θ_{uR} is an angle in the rotation matrix V_{uR} to diagonalize $I_{RL}^{(00)} U_4 U_4^\dagger I_{RL}^{(00)}$:

$$\tan 2\theta_{uR} = \frac{2(a^2 - b^2)cd \sin \theta' \cos \theta'}{c^2(a^2 \cos^2 \theta' + b^2 \sin^2 \theta') - d^2(a^2 \sin^2 \theta' + b^2 \cos^2 \theta')} . \quad (4.19)$$

The constant α_s should be estimated at the scale $\mu_D = 2.8 \text{ GeV}$ where the $\Delta C = 2$ process is actually measured [21]. So we have to take into account the renormalization group effect from the weak scale down to μ_D :

$$\alpha_s^{-1}(\mu_D) = \alpha_s^{-1}(M_Z) - \frac{1}{6\pi} \left(23 \ln \frac{M_Z}{m_b} + 25 \ln \frac{m_b}{\mu_D} \right) \longrightarrow \alpha_s(\mu_D) \approx 0.240 \quad (4.20)$$

where $\alpha_s(M_Z) \approx 0.1184$ has been put.

Similarly, the effective Hamiltonian of LL type (4.7) and the RR type (4.8) are respectively rewritten;

$$-\frac{\pi\alpha_s}{2}(\alpha_u + \alpha'_u)^2 R^2 S_{KK}^{LL} \cdot \frac{4}{3} Q_1 , \quad -\frac{\pi\alpha_s}{2} \sin^2 2\theta_{uR} R^2 S_{KK}^{RR} \cdot \frac{4}{3} \tilde{Q}_1 , \quad (4.21)$$

where

$$S_{KK}^{LL} = S_{KK}^{RR} = \pi R \sum_{n=1}^{\infty} \frac{1}{n^2} \left(I_{RR}^{1(0n0)} - I_{RR}^{2(0n0)} \right)^2 . \quad (4.22)$$

Combining these results we obtain the lower bounds for the compactification scale from the constraint (4.12). First let us assume that only one of the three types of diagrams (LL, RR, LR) gives dominant contribution to the mixing. Then we get lower bound on the compactification scale by use of the upper bound on the relevant coefficients z_1, z'_1 and z_4 given in (4.12):

$$\begin{cases} |z_1| : R^{-1} \gtrsim 9.39 |\alpha_u + \alpha'_u| \sqrt{S_{KK}^{LL}} \times 10^2 [\text{TeV}] , \\ |\tilde{z}_1| : R^{-1} \gtrsim 9.39 |\sin 2\theta_{uR}| \sqrt{S_{KK}^{RR}} \times 10^2 [\text{TeV}] , \\ |z_4| : R^{-1} \gtrsim 5.19 \sqrt{|(\alpha_u + \alpha'_u) \sin 2\theta_{uR} S_{KK}^{LR}|} \times 10^3 [\text{TeV}] . \end{cases} \quad (4.23)$$

Let us note that LR type diagram yields both of Q_4 and Q_5 operators as is seen in (4.13). We, however, can safely ignore the contribution of Q_5 to the mixing, because in (4.13) the coefficient of the operator is smaller than that of Q_4 and also because the magnitude of the hadronic matrix element of Q_4 is known to be greater than that of Q_5 , as the constraint for z_4 is more severe than that for z_5 in (4.12). This is why we used the constraint for z_4 alone to get the lower bound for the case of LR type diagram. Since our theory has one free parameter, say θ' , each lower bound on R^{-1} depends on it. The obtained numerical results are given in Fig. 2, where the lower bound on R^{-1} is plotted as a function of $\sin \theta'$ for each type of diagram.

Now we learn from Fig. 2 that the contribution of LR type diagram is always negligible. Thus we can combine the contributions to the mixing from LL and RR type diagrams

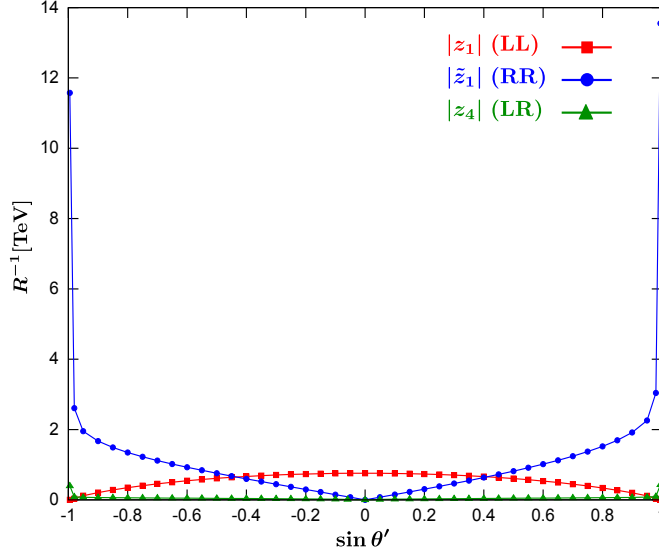


Figure 2: Lower bounds on R^{-1} as a function of $\sin \theta'$ obtained for each of 3 types of diagrams.

together in order to get real lower bound on the compactification scale. Namely, by use of the fact $\langle \bar{D}^0 | Q_1 | D^0 \rangle = \langle \bar{D}^0 | \tilde{Q}_1 | D^0 \rangle$ (due to the parity symmetry of strong interaction) we can sum up the coefficients for Q_1 and \tilde{Q}_1 shown in (4.21) together and can utilize the constraint for z_1 (or equally for \tilde{z}_1) to get the bound for R^{-1} :

$$R^{-1} \gtrsim 9.39 \sqrt{\left\{ (\alpha_u + \alpha'_u)^2 + \sin^2 2\theta_{uR} \right\} S_{\text{KK}}^{LL}} \times 10^2 [\text{TeV}], \quad (4.24)$$

where $S_{\text{KK}}^{LL} = S_{\text{KK}}^{RR}$ is understood. Such obtained lower bound for R^{-1} is displayed in Fig. 3.

If we require that the prediction of our model is consistent with data, irrespectively of the choice of θ' , we get the most stringent bound on the compactification scale, which should be the possible largest value in Fig. 3, i.e. $R^{-1} \gtrsim 14 \text{ TeV}$. However, the most stringent bound comes from the very extreme case $|\sin \theta'| \simeq 1$. For $|\sin \theta'| \lesssim 0.4$, the LL type contribution is dominant and provides a mild lower bound 0.8 TeV. As for the other range of θ' except for the case $|\sin \theta'| \simeq 1$, the RR type contribution is dominant and the lower bound becomes around $\mathcal{O}(1 \text{ TeV})$ depending on the value of θ' .

A few comments are in order. Fig. 2 indicates that the lower bounds obtained from the LR and the RR type contributions vanish at $\sin \theta' = 0$. In this case, we see the Yukawa coupling for up-type quarks becomes diagonal: $\theta_{uL} = \theta_{uR} = 0$. Thus in this extreme case the up type quark mixings disappear and the contributions of KK gluon exchange accidentally vanish for these two types of diagram. Note, however, that the lower bound obtained from the LL type contribution does not vanish even though $\theta_{uL} = 0$. This is because θ in (3.9) relevant for down-type quark mixing also contributes to the left-handed FCNC current as is seen in (4.16). Namely, because of the mixing between Q_{3L} and Q_{6L} ,

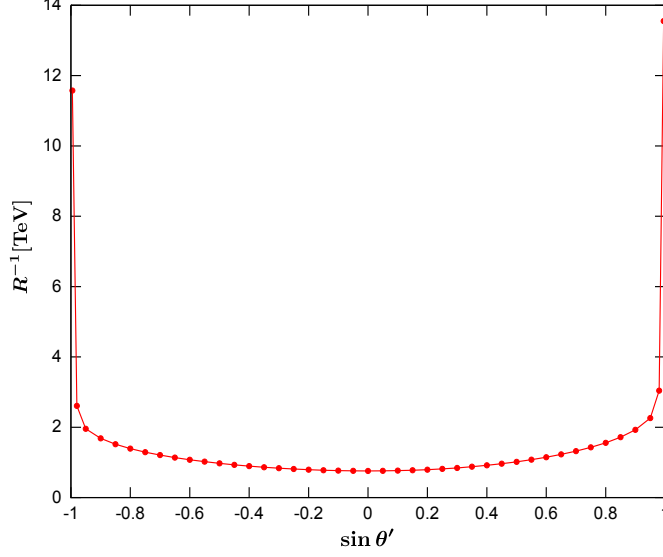


Figure 3: Lower bound on R^{-1}

U_3 also contributes to the FCNC vertex (4.4), which is non-diagonal even for $\theta' = 0$. Thus even in the case of $\sin \theta' = 0$ we get a meaningful lower bound on M_c (see Fig. 3).

5 Suppression mechanism of FCNC

Note that the obtained lower bounds are smaller than what we naively expect assuming that the tree level diagram relevant for the FCNC process is simply suppressed by $1/M_c^2$ [21]:

$$\frac{1}{M_c^2} \lesssim 10^{-6} [\text{TeV}^{-2}] \quad \longrightarrow \quad M_c \gtrsim \mathcal{O}(10^3) [\text{TeV}] , \quad (5.1)$$

which is much more stringent than the lower bound we obtained except for the extreme case of $|\sin \theta'| \simeq 1$.

This apparent discrepancy may be attributed to a suppression mechanism in our scenario, which we will see now. The rate of $D^0 - \bar{D}^0$ mixing is handled by the factor $(I_{RR}^{1(0n0)} - I_{RR}^{2(0n0)})^2$ as is seen in S_{KK}^{LR} and S_{KK}^{LL} , which is sensitive to the non-universality of gauge coupling of KK gluons coming from the difference of bulk masses ($M^1 \neq M^2$). It is easy to see that this factor is automatically suppressed for generations with light quarks such as 1st and 2nd generations.

Recall that in GHU hierarchical small quark masses are naturally realized without fine tuning by exponential suppression factors $e^{-\pi R M^i}$ with $\pi R M^i \gg 1$. On the other hand, when $\pi R M^i \gg 1$, the “width” $1/M^i$ of the mode function of zero-mode fermion is much smaller than the period $\frac{2\pi R}{n}$ of KK gauge boson mode functions $\cos(\frac{n}{R}y)$.⁸ Then

⁸ Note that KK modes with relatively small n play an important role in the convergent mode sum \sum_n .

the exponential dumping of the fermion mode functions is so fast that the mode functions of KK gauge bosons behave as almost constant in the overlap integral. Thus the situation mimics the interaction vertex for zero-mode gauge boson and the gauge coupling of KK gauge bosons becomes almost universal. Therefore FCNC processes at the tree level should be automatically suppressed for the processes with respect to the light quarks by this mechanism.

In fact, analytic calculations of the mode sum in $S_{\text{KK}}^{LL(RR),LR}$ give approximate expressions for the limit $\pi R M^i \gg 1$,

$$S_{\text{KK}}^{LL} \simeq \frac{\pi^2}{4} \frac{(\mu - \nu)^2}{\mu\nu(\mu + \nu)} , \quad (5.2)$$

$$S_{\text{KK}}^{LR} \simeq -\pi^2 \left\{ \frac{e^{-\mu} + e^{-\nu}}{2} - \frac{\mu^2 + \nu^2 - \mu\nu}{\mu\nu(\mu - \nu)} (e^{-\nu} - e^{-\mu}) \right\} . \quad (5.3)$$

where $\mu \equiv 2\pi R M^1$ and $\nu \equiv 2\pi R M^2$. A remarkable thing here is that S_{KK}^{LL} (S_{KK}^{RR}) is suppressed by an inverse power of M^i , while S_{KK}^{LR} is exponentially suppressed. Thus the suppression of FCNC is much more severe for the contribution of the LR type diagram. This is the reason why the contribution of the LR type diagram is always much smaller than those of LL and RR type diagrams for any value of $\sin \theta'$. We may understand qualitatively why S_{KK}^{LR} is much smaller than S_{KK}^{LL} as follows. Let us note that the mode sum in S_{KK}^{LR} ,

$$\sum_{n=1}^{\infty} \frac{(-1)^n}{n^2} = \sum_{n=1}^{\infty} \left\{ \frac{1}{(2n)^2} - \frac{1}{(2n-1)^2} \right\} = \sum_{n=1}^{\infty} \frac{-4n+1}{(2n)^2(2n-1)^2} , \quad (5.4)$$

behaves as $\sim -\frac{1}{4} \sum \frac{1}{n^3}$ for larger n . Thus the convergence of S_{KK}^{LR} is faster than that of S_{KK}^{LL} . That means in the mode sum in S_{KK}^{LR} only smaller integer of n contributes to the sum and therefore the validity of the approximation $1/M^i \ll \frac{2\pi R}{n}$ to ensure the universality of gauge couplings is much better in S_{KK}^{LR} than in S_{KK}^{LL} .

We may say that the suppression mechanism for the case of LR type contribution is similar to the famous GIM-mechanism where FCNC is suppressed by a typical factor $\frac{m_s^2 - m_d^2}{M_W^2}$, since $e^{-\mu} \sim \frac{m_d^2}{M_W^2}$ ($\mu = 2\pi R M^1$) etc. Thus it is reasonable to call this suppression mechanism ‘‘GIM-like’’.⁹

In the exceptional extreme case $|\sin \theta'| \simeq 1$, the bulk mass M^2 happens to be relatively small and these suppression mechanisms do not work. That is why we get the severe lower bound on the compactification scale in the extreme case.

6 Summary

In this paper, we have discussed the flavor mixing and the resulting flavor changing neutral current (FCNC) processes in the framework of five dimensional $SU(3) \otimes SU(3)_{\text{color}}$ gauge-

⁹A GIM mechanism for suppression of flavor violation was known and well studied in warped space models [22].

Higgs unification scenario. As the FCNC process, in this paper we have discussed $D^0 - \bar{D}^0$ mixing in the light of the recent progress in the measurements of $D^0 - \bar{D}^0$ mixing, which is known to be induced by the exchange of non-zero KK gluons at the tree level.

The gauge-Higgs sector in the scenario is governed by gauge principle and therefore is very predictive, as is seen in the case of Higgs mass, whose radiative correction is guaranteed to be finite by the higher dimensional gauge symmetry regardless of the non-renormalizability of the theory [2]. On the other hand, understanding the flavor physics in the fermion sector is a challenging issue since Yukawa coupling is originated from the (flavor universal) gauge coupling.

In our previous paper discussing $K^0 - \bar{K}^0$ mixing [11], we have shown that how flavor mixings are realized in the scenario. In the present paper we have stressed that flavor mixing is due to the interplay between the bulk masses and the brane localized masses. Namely by suitable unitary transformations of fermion we can always take the basis where the origin of flavor mixing is solely attributed to either of bulk mass term or brane localized mass term. Thus physical flavor mixing stems only when we cannot “diagonalize” both of bulk and brane localized mass term simultaneously. This suggests that once bulk masses get degenerated simultaneous diagonalization becomes possible and the flavor mixing of the theory completely disappears in this limit. We have confirmed this important property by explicit calculation. In this way, in our model of gauge-Higgs unification the “new physics” contributions, namely all contributions of non-zero KK modes to FCNC, disappear for the limit of degenerate bulk masses.

The above argument implies that FCNC is under control by the mass-squared difference of quarks, just as in the case of the standard model where $D^0 - \bar{D}^0$ mixing is handled by $\frac{m_s^2 - m_d^2}{M_W^2}$ coming from the box diagram for the simplified 2 generation case: the famous GIM mechanism. To be more precise, the situation is a little different in these two kinds of theory. Namely, in our model Cabibbo angle and therefore all FCNC disappear for degenerate bulk masses, $c = d$ in (3.10), even if $m_d \neq m_s$. On the other hand, the limit $c = d$ corresponds to the limit where averaged squared-masses of quarks get degenerated between the first and the second generations, i.e. $m_d^2 + m_u^2 = m_s^2 + m_c^2$ (see for instance e.g. (3.13) to (3.16)). Thus FCNC due to the exchange of non-zero KK gluons at the tree level is controlled by

$$\frac{(m_s^2 + m_c^2) - (m_d^2 + m_u^2)}{M_W^2}, \quad (6.1)$$

while the box diagram due to the exchange of zero-mode charged gauge boson is also handled by $\frac{m_s^2 - m_d^2}{M_W^2}$ just as in the standard model.

The fact that $D^0 - \bar{D}^0$ mixing is handled by the mass-squared difference of quarks in our model suggests that we have a suppression mechanism of FCNC, similar to GIM mechanism, even for the contribution of KK gluon exchange. In fact we have shown that the amplitude of KK gluon exchange is suppressed concerning the contribution of

light quarks of first and second generations. The reason of the suppression was argued to be the approximate universality of gauge couplings of KK gluons for light quarks and the suppression also has been found to really happen in the $D^0 - \bar{D}^0$ mixing by explicit analytic calculations. Interestingly, the extent of the suppression turns out to be different for two kind of Feynman diagrams contributing to the gluon exchange, i.e. LR type diagram “with chirality flip” and LL or RR type diagrams “without chirality flip”. To be more concrete, the suppression in the LR type diagram is exponential suppression by the factors $e^{-2\pi RM^1}$, $e^{-2\pi RM^2}$, while the suppression in the LL or RR type diagrams is only by the inverse powers of large bulk masses, $\frac{1}{2\pi RM^{1,2}}$. Since small quark masses are naturally realized by the exponential suppression in the gauge-Higgs unification scenario, i.e. $\frac{m_d^2}{M_W^2} \sim e^{-2\pi RM^1}$, etc., the suppression in the case of LR type diagram is similar to the well-known GIM mechanism and we have called it “GIM-like” mechanism. We also have discussed the origin of such qualitative difference of two suppression mechanisms.

We have shown that although the condition by Glashow-Weinberg [15] is satisfied in good approximation for the zero-mode sector of quarks, we still have FCNC at the tree level because of the presence of new source of flavor violation, i.e. the non-degenerate bulk masses as a new feature of the gauge-Higgs unification scenario.

The rate of $D^0 - \bar{D}^0$ mixing at the tree level via KK gluon exchange has been calculated. The obtained result for the mass difference of neutral D meson is suppressed by the inverse powers of compactification scale $M_c = R^{-1}$ (the decoupling effects of heavy non-zero KK gluons). The contributions from the diagrams without chirality flip (LL and RR) turn out to be dominant. Then by use of the constraints on the Wilson coefficients of relevant 4-Fermi effective operators [19] obtained from the recent measurements of the mass difference by BABAR and Bell experiments we have obtained the lower bounds on the compactification scale as the prediction of our model. Though the result depends on a free parameter θ' , it is of order $\mathcal{O}(\text{TeV})$ for almost all range of θ' . The obtained lower bound is much milder than we naively expect assuming only the decoupling of KK gluons and should be the reflection of the presence of the suppression mechanism of FCNC, mentioned above.

In the appendix we re-analyze $K^0 - \bar{K}^0$ mixing including the contributions of LL and RR type diagrams in addition to the one of LR type diagram calculated in our previous paper [11]. As is seen there the obtained lower bound on the compactification scale is much more severe in the case of $K^0 - \bar{K}^0$ mixing. Such difference should be attributed to the difference of the factor of flavor mixing in the vertices of KK gluons for up-type and down-type quarks. The origin of such difference should be the difference of up-type and down-type quark masses, since we easily find that in the imaginative limit of degenerate up- and down-type quark masses, $a = b = \frac{1}{\sqrt{2}}$, such difference disappears. We, however, have not completely understood qualitatively why such difference of the order of magnitude in the obtained lower bounds for $K^0 - \bar{K}^0$ and $D^0 - \bar{D}^0$ mixings arises.

Finally we briefly comment on other closely related typical FCNC and CP violating observables in our model: i.e. $B^0-\bar{B}^0$ mixing and CP violating parameter ϵ in the neutral K system.

Concerning $B^0-\bar{B}^0$ mixing, expanding our model in order to include the third generation is clear necessary. A serious issue is how to implement the t quark mass, since the bulk mass is effective only for light quarks. It has been pointed out that to introduce 4-th rank symmetric repr. of SU(3), i.e. 15 repr. is necessary to get $m_t \simeq 2M_W$ [23]. Still remaining small gap $m_t - 2M_W$ is argued to be attributed to the quantum correction. Interestingly, in our framework the large gap between m_t and m_b and small generation mixings between the third generation and lighter generation seems to be inevitable consequences. Namely, for the third generation the bulk mass is not needed $M_3 = 0$, as it only works to reduce the quark masses. Still the relation $m_t^2 + m_b^2 = (2M_W)^2$ (at the tree level) implies that in order to guarantee $m_t \simeq 2M_W$, m_b inevitably becomes much smaller than m_t in accordance with reality. Also to keep $m_t \simeq 2M_W$, the mixing between the third generation and lighter generations should be small, since such mixing tends to reduce the t quark mass. In this way, the large top quark mass seems to lead to the desirable pattern of quark masses and generation mixings. Thus in the 0-th order approximation, U_3 , U_4 in (3.2) for the three generation model looks like

$$U_4 = \begin{bmatrix} \cos \theta' & -\sin \theta' & 0 \\ \sin \theta' & \cos \theta' & 0 \\ 0 & 0 & 1 \end{bmatrix} \begin{bmatrix} a & 0 & 0 \\ 0 & b & 0 \\ 0 & 0 & c \end{bmatrix}, \quad (6.2)$$

$$U_3 = \begin{bmatrix} \cos \theta & -\sin \theta & 0 \\ \sin \theta & \cos \theta & 0 \\ 0 & 0 & 1 \end{bmatrix} \begin{bmatrix} \sqrt{1-a^2} & 0 & 0 \\ 0 & \sqrt{1-b^2} & 0 \\ 0 & 0 & \sqrt{1-c^2} \end{bmatrix}. \quad (6.3)$$

where the parameter c is very close to 1, $c \simeq 0.9983$. Thus the third generation is isolated from remaining generations and clearly $B^0-\bar{B}^0$ mixing disappears in this limit. This argument implies that even though the $B^0-\bar{B}^0$ mixing arises after the inclusion of small mixings between the third generation and lighter generations, the rate of the FCNC process is suppressed by the small mixings and the lower bound on the compactification scale obtained from the comparison of the prediction of our model with the data is expected not to exceed that obtained from $D^0-\bar{D}^0$ mixing or $K^0-\bar{K}^0$ mixing discussed in this paper.

In the analysis of ϵ in the neutral K system, inclusion of CP violating parameter, so far ignored, is clearly needed. In the base where the bulk mass term is diagonalized, only source of the CP phase will be in U_3 and U_4 in (3.2). Interestingly, in our model the CP phase seems to remain even in the two generation scheme. Namely the most general form of U_3 and U_4 in the two generation scheme is known to be given as

$$U_4 = \begin{bmatrix} \cos \theta' & -\sin \theta' \\ \sin \theta' & \cos \theta' \end{bmatrix} \begin{bmatrix} a & 0 \\ 0 & b \end{bmatrix}, \quad U_3 = \begin{bmatrix} \cos \theta & -\sin \theta \\ \sin \theta & \cos \theta \end{bmatrix} \begin{bmatrix} 1 & 0 \\ 0 & e^{i\delta} \end{bmatrix} \begin{bmatrix} \sqrt{1-a^2} & 0 \\ 0 & \sqrt{1-b^2} \end{bmatrix}. \quad (6.4)$$

where the CP violating phase δ does not need to appear in U_3 but may appear in U_4 if we wish. The important observation is that by generalizing the rotation matrices in the left of U_3 , U_4 used in the analysis of $D^0-\bar{D}^0$ and $K^0-\bar{K}^0$ mixings to unitary matrices, we first get 3 phases in each of U_3 , U_4 , but after rephasing of Q_3 , Q_6 and Q_{SM} there remains only one physical CP violating phase, which we wrote δ . Let us note that an overall phase of Q_3 , Q_6 and Q_{SM} is irrelevant in the reduction of the number of phases. Thus it turns out that the KK gluon vertex of the LL type contains the CP violating phase, since it gets contributions from both of U_3 and U_4 . Thus this vertex is expected to give the imaginary part in the amplitude of $K^0-\bar{K}^0$ mixing through KK gluon exchange at the tree level, and therefore to the parameter ϵ . We do not perform the detailed calculation of ϵ here, but the comparison of our prediction with the data of ϵ will be another interesting issue to be addressed in order to get meaningful constraints on the compactification scale and/or the CP phase δ .

Acknowledgments

This work was supported in part by the Grant-in-Aid for Scientific Research of the Ministry of Education, Science and Culture, No. 21244036.

A The constraint from $K^0-\bar{K}^0$ mixing

We discuss the constraint on the compactification scale R^{-1} obtained from the analysis of $K^0-\bar{K}^0$ mixing. The contribution of non-zero KK gluon exchange processes is dominant in this case [11]. In the previous analysis [11], we have considered only the LR type diagram shown in the Fig.4(i). This is because we expected that the contribution of this diagram was dominant due to the chiral enhancement factor $\frac{m_K}{m_d+m_s}$ in the hadronic matrix element under our assumption that the mode sums $S_{KK}^{LL}(=S_{KK}^{RR})$ and S_{KK}^{LR} given in (A.1) are more or less of the same order of magnitude. However, it turns out that we have to take into account the other contributions from the LL and the RR type diagrams as well, since the above naive assumption on the mode sum is not correct as the matter of fact, $S_{KK}^{LL} \gg S_{KK}^{LR}$. Therefore, we re-analyze $K^0-\bar{K}^0$ mixing in this appendix.

The contributions to K_L-K_S mass difference $\Delta m_K(\text{KK})$ from each type of diagrams shown in Fig.4 are given as follows, respectively;

$$\begin{aligned}\Delta m_K^{LR}(\text{KK}) &= 2\pi\alpha_s R^2 \left(B_4 - \frac{B_5}{9}\right) \left(\frac{m_K}{m_d+m_s}\right)^2 f_K^2 m_K \sin 2\theta_{dR} (\alpha_d + \alpha'_d) S_{KK}^{LR}, \\ \Delta m_K^{LL}(\text{KK}) &= -\frac{4}{9}\pi B_1 \alpha_s R^2 f_K^2 m_K (\alpha_d + \alpha'_d)^2 S_{KK}^{LL}, \\ \Delta m_K^{RR}(\text{KK}) &= -\frac{4}{9}\pi B_1 \alpha_s R^2 f_K^2 m_K \sin^2 2\theta_{dR} S_{KK}^{LL}.\end{aligned}\tag{A.1}$$

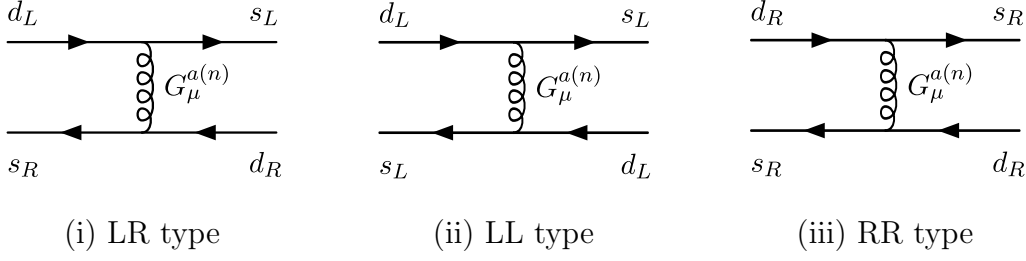


Figure 4: The diagrams of $K^0 - \bar{K}^0$ mixing via KK gluon exchange

where

$$\begin{aligned}\alpha_d &\equiv -(1 - a^2) \sin 2\theta_{dL} \cos^2 \theta + (1 - b^2) \sin 2\theta_{dL} \sin^2 \theta - \sqrt{(1 - a^2)(1 - b^2)} \cos 2\theta_{dL} \sin 2\theta, \\ \alpha'_d &\equiv -a^2 \sin 2\theta_{dL} \cos^2 \theta' + b^2 \sin 2\theta_{dL} \sin^2 \theta' - ab \cos 2\theta_{dL} \sin 2\theta'.\end{aligned}\quad (\text{A.2})$$

θ_{dR} is an angle in the rotation matrix V_{dR} to diagonalize $I_{RL}^{(00)} U_3 U_3^\dagger I_{RL}^{(00)}$:

$$\tan 2\theta_{dR} = \frac{2(b^2 - a^2)cd \sin \theta \cos \theta}{(1 - a^2)c^2 - (1 - b^2)d^2 + (a^2 - b^2)(c^2 + d^2) \sin^2 \theta}.\quad (\text{A.3})$$

The bag parameters are calculated by lattice simulation as $B_1 = 0.57$, $B_4 = 0.81$ and $B_5 = 0.56$ [24]. $f_K (\simeq 1.23 f_\pi)$, m_K is the kaon decay constant and the kaon mass, respectively. The constant α_s is estimated to be $\alpha_s(\mu_K) \approx 0.268$ for $\mu_K = 2.0 \text{ GeV}$ [24]. Combining these results, we obtain

$$\begin{aligned}\Delta m_K(\text{KK}) &\sim -1.61 \times 10^2 \cdot (R f_\pi)^2 \\ &\times \left[\left\{ (\alpha_d + \alpha'_d)^2 + \sin^2 2\theta_{dR} \right\} S_{\text{KK}}^{LL} - 65.0 \cdot \sin 2\theta_{dR} (\alpha_d + \alpha'_d) S_{\text{KK}}^{LR} \right] [\text{MeV}]\end{aligned}\quad (\text{A.4})$$

The room for the “New Physics” contribution $\Delta m_K(\text{NP})$ is basically given by the difference between the experimental data and the standard model prediction [25], [26]. Though the short-distance contribution due to the box diagram in the standard model [25] is reliably calculated the long-distance contribution has uncertainty. Thus here we take an attitude that $\Delta m_K(\text{NP})$ can be as large as the experimental value:

$$|\Delta m_K(\text{NP})| < \Delta m_K(\text{Exp}) = 3.48 \times 10^{-12} [\text{MeV}]\quad (\text{A.5})$$

Identifying $\Delta m_K(\text{NP})$ with our result $\Delta m_K(\text{KK})$ we obtain a lower bound for the compactification scale:

$$R^{-1} \gtrsim 6.32 \times 10^2 \sqrt{\left\{ (\alpha_d + \alpha'_d)^2 + \sin^2 2\theta_{dR} \right\} S_{\text{KK}}^{LL} - 65.0 \cdot \sin 2\theta_{dR} (\alpha_d + \alpha'_d) S_{\text{KK}}^{LR}} [\text{TeV}].\quad (\text{A.6})$$

The obtained numerical result is given in Fig. 5 where the first term inside the square root in (A.6) is dominant. The lower bound on the compactification scale R^{-1} ranges from 2.8 TeV to 43 TeV depending on the value of $\sin \theta'$.

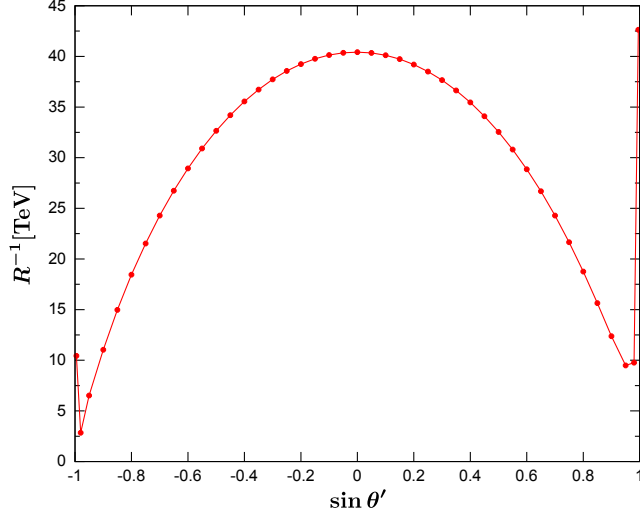


Figure 5: Lower bounds on R^{-1} obtained from the data on $K^0-\bar{K}^0$ mixing.

References

- [1] N. S. Manton, Nucl. Phys. B **158**, 141 (1979);
D. B. Fairlie, Phys. Lett. B **82**, 97 (1979), J. Phys. G **5**, L55 (1979);
Y. Hosotani, Phys. Lett. B **126**, 309 (1983), Phys. Lett. B **129**, 193 (1983), Annals Phys. **190**, 233 (1989).
- [2] H. Hatanaka, T. Inami and C. S. Lim, Mod. Phys. Lett. A **13**, 2601 (1998).
- [3] I. Antoniadis, K. Benakli and M. Quiros, New J. Phys. **3**, 20 (2001);
G. von Gersdorff, N. Irges and M. Quiros, Nucl. Phys. B **635**, 127 (2002);
R. Contino, Y. Nomura and A. Pomarol, Nucl. Phys. B **671**, 148 (2003);
C. S. Lim, N. Maru and K. Hasegawa, J. Phys. Soc. Jap. **77**, 074101 (2008).
- [4] K. Hasegawa, C. S. Lim and N. Maru, Phys. Lett. B **604**, 133 (2004).
- [5] N. Maru and T. Yamashita, Nucl. Phys. B **754**, 127 (2006);
Y. Hosotani, N. Maru, K. Takenaga and T. Yamashita, Prog. Theor. Phys. **118**, 1053 (2007).
- [6] C. S. Lim and N. Maru, Phys. Rev. D **75**, 115011 (2007).
- [7] N. Maru and N. Okada, Phys. Rev. D **77**, 055010 (2008);
N. Maru, Mod. Phys. Lett. A **23**, 2737 (2008).
- [8] Y. Adachi, C. S. Lim and N. Maru, Phys. Rev. D **76**, 075009 (2007); Phys. Rev. D **79**, 075018 (2009).
- [9] Y. Adachi, C. S. Lim and N. Maru, Phys. Rev. D **80**, 055025 (2009).

- [10] C. S. Lim, N. Maru and K. Nishiwaki, Phys. Rev. D **81**, 076006 (2010).
- [11] Y. Adachi, N. Kurahashi, C. S. Lim and N. Maru, JHEP **0809**, 1011 (2010) 150.
- [12] D. E. Kaplan and T. M. P. Tait, JHEP **0111**, 051 (2001).
- [13] G. Burdman and Y. Nomura, Nucl. Phys. B **656**, 3 (2003).
- [14] A. Delgado, A. Pomarol and M. Quiros, JHEP **0001**, 030 (2000).
- [15] S. L. Glashow and S. Weinberg, Phys. Rev. D **15**, 1958 (1977).
- [16] E. Barberio et al. (Heavy Flavor Averaging Group), arXiv:0808.1297.
- [17] K. Agashe, R. Contino and A. Pomarol, Nucl. Phys. B **719**, 165 (2005).
- [18] C. A. Scrucca, M. Serone and L. Silvestrini, Nucl. Phys. B **669**, 128 (2003).
- [19] O. Gedalia, Y. Grossman, Y. Nir and G. Perez, Phys. Rev. D **80**, 055024 (2009).
- [20] C. Csaki, A. Falkowski, A. Weiler, Phys. Rev. **D80**, 016001 (2009).
- [21] M. Bona *et al.* [UTfit Collaboration], JHEP **0803**, 049 (2008).
- [22] T. Gherghetta and A. Pomarol, Nucl. Phys. B **586**, 141 (2000);
S. J. Huber, Nucl. Phys. B **666**, 269 (2003);
K. Agashe, G. Perez and A. Soni, Phys. Rev. D **71**, 016002 (2005).
- [23] G. Cacciapaglia, C. Csaki and S. C. Park, JHEP **0603**, 099 (2006).
- [24] M. Blanke, A. J. Buras, B. Duling, S. Gori and A. Weiler, JHEP **0903**, 001 (2009).
- [25] T. Inami and C.S. Lim, Prog. Theor. Phys. **65**, 297 (1981).
- [26] I. I. Bigi and A. I. Sanda “CP Violation”, Cambridge University Press (2000).